Available online at www.dergipark.org.tr/en

INTERNATIONAL ADVANCED RESEARCHES and ENGINEERING JOURNAL

Journal homepage: www.dergipark.org.tr/en/pub/iarej

e-ISSN: 2618-575X

International Open Access

Volume 05
Issue 02

August, 2021

Research Article

Numerical assessment of the performance of different constitutive models used to predict liquefiable soil behavior

Selçuk Demir [a,*]

[a]*Bolu Abant İzzet Baysal University, Engineering Faculty, Department of Civil Engineering, 14030, Bolu, Turkey*

ARTICLE INFO

Article history:
Received 01 February 2021
Revised 27 April 2021
Accepted 14 May 2021

Keywords:
DeepSoil
Liquefaction
MKZ Model
OpenSees
PDMY02 Model

ABSTRACT

Liquefaction has caused severe damages to structures such as excessive settlements, tilting, lateral spreading etc., all over the world during many past earthquakes. Hence, the efficient prediction of liquefiable soil behavior is crucial for liquefaction-induced hazard evaluation of existing structures and the design of new structures in seismically active regions. In this study, a series of nonlinear effective stress analyses are carried out using the DeepSoil and OpenSees opensource software with Modified Kondner–Zelasko (MKZ) and Pressure Dependent Multi Yield02 (PDMY02) constitutive models to evaluate their capabilities in terms of predicting liquefiable soil behavior. The performance of the models has been evaluated by comparing the results between the numerical predictions and a centrifuge study from literature in terms of excess pore water pressures, acceleration-time histories, spectral accelerations, lateral displacements and maximum profile responses at specific depths. The results clearly illustrate that the excess pore water pressure predictions from nonlinear analyses are reasonably close to centrifuge measurements, but the accelerations and lateral displacements are slightly different. It is also observed that dissimilarities in the predictions of the numerical simulations are more obvious for OpenSees simulations with respect to DeepSoil ones.

1. Introduction

Soil liquefaction is a complex phenomenon that has been observed in many historical earthquakes in its various aspects [1]. When a soil deposit is liquefied, the excess pore pressures in the soil become equal to the effective stress of soil then the strength and stiffness of the soil reduce dramatically. Different consequences of soil liquefaction may be seen during and after an earthquake such as excessive settlements, tilting, and lateral spreading [2]. These consequences are the main reasons behind the massive damage to structures and life.

A wide range of case studies, experimental tests, or numerical models have been employed in recent years to highlight soil liquefaction and its effects on structures. Evaluation of liquefiable soil behavior with experimental tests may be thought an ideal method under realistic earthquake conditions. However, these tests are generally costly and too complex to put into practice. On the other hand, numerical analysis or modeling offers an economical solution to simulate soil behavior with different parametric variables.

Reliable prediction of the behavior of a liquefiable soil profile (i.e., excess pore pressures, accelerations, and deformations) remains a major challenge in geotechnical earthquake engineering. In this regard, numerical modeling is an efficient tool for practitioners to predict liquefiable soil behavior and prevent liquefaction-induced failures in the future. Provided that constitutive soil models sufficiently cover the real soil behavior under seismic loading, the liquefiable soil behavior can be reasonably simulated via numerical studies. In other words, considerable attention is needed during the calibration of constitutive soil models in order to properly represent the soil nonlinearity.

A key issue of assessing the accuracy of a numerical simulation is to compare results of the case history or experiment data with computed results. In recent decades,

* Corresponding author. Tel.: +90-374-254-4831; Fax: +90-374-253-4558.
E-mail address: selcukdemir@ibu.edu.tr *(S. Demir)*
ORCID: 0000-0003-2520-4395 *(S. Demir)*
DOI: 10.35860/iarej.871429

researchers have been performed numerous numerical efforts using dynamic centrifuge model test results [3-7] to predict the liquefiable soil behavior due to the increasing availability of computational resources and constitutive soil models [8-16].

Popescu and Prevost [3] and Byrne et al. [4] presented the comparison of numerical modeling predictions using constitutive soil models and measured centrifuge model response to investigate soil liquefaction. Also, Taiebat et al. [5] presented numerical analysis results of a liquefiable sand using two types of plasticity models. They concluded that the capabilities of the two numerical models producing pore pressures in the liquefiable sand are consistent with observations of the centrifuge test. Ramirez et al. [6] investigated the predictive capabilities of two constitutive soil models namely PDMY02 (OpenSees) and SANISAND (Flac) by using element tests and centrifuge test results in a liquefiable soil profile. They concluded that although PDMY02 and SANISAND models are capable of predicting excess pore pressures and accelerations, liquefaction induced volumetric settlements still remain poorly. Demir and Özener [7] numerically simulated a centrifuge test with UBC3D-PLM model implemented in Plaxis and their results showed that excess pore water pressure development and time history of accelerations are consistent with experimental observations, unlike excess pore pressure dissipation and displacements.

This paper aims to study the capabilities of the MKZ and PDMY02 soil constitutive models for predicting the one-layered liquefiable soil behavior and provide a calibration guide of the two numerical models for accurate modeling of liquefiable soils. To this end, a numerical study was carried out in open-source software DeepSoil and OpenSees. Results of numerical simulations have been compared with results of a centrifuge test from the literature. At the end of the simulations, the performance of numerical models is discussed.

2. Details of Numerical Modeling

Performance of the numerical models was investigated through results of a centrifuge test conducted on saturated liquefiable soil by Taboada and Dobry [17] during the VELACS project (Model No: 1). Figure 1 shows a schematic representation of the laminar box, including instrumentations used during the centrifuge test. One-layered uniform Nevada Sand (D_r = 40%) with 10 m thick was adopted in the centrifuge study. The groundwater table (GWT) was located at the ground surface. The laminar box was subjected to a centrifuge acceleration of 50 g. A sinusoidal input motion with a maximum value of 0.235g shown in Figure 1(b) was excited during the test. Pore water pressures, accelerations, and horizontal displacements were recorded in different locations during the centrifuge test using piezometers (P), horizontal accelerometers (AH), and horizontal displacement transducers (LVDT), respectively.

Two different open-source computational platforms were chosen for this study, DeepSoil and OpenSees. The Pressure Dependent Modified Kondner–Zelasko (MKZ) and Pressure Dependent Multi-Yield02 (PDMY02) nonlinear constitutive soil models were considered in DeepSoil and OpenSees simulations, respectively. Details of the modeling procedures of constitutive models were described below. Figure 2 simply shows the simulated soil profile for two numerical models.

2.1 DeepSoil

Nonlinear analyses were employed using the software DeepSoil v7.0 [18]. The soil column was discretized one-dimensionally (1D) as a multi-degree-of-freedom (MDOF) lumped mass model. Each layer was represented by a corresponding mass, a nonlinear spring, and a dashpot. The nonlinear soil behavior was modeled using pressure-dependent Modified Kondner–Zelasko (MKZ) hyperbolic-type model with non-Masing hysteretic Re/Un-loading formulation. MKZ model developed by Matasovic and Vucetic [19] is a widely preferred nonlinear soil model in order to define the soil backbone characteristic and cyclic loading-unloading behavior. In DeepSoil simulations, a frequency-independent viscous damping formulation proposed by Phillips and Hashash [20] was used to represent small-strain damping.

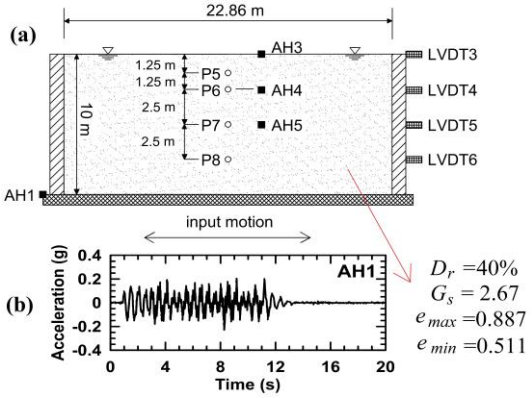

Figure 1. (a) Illustration of the centrifuge test (Model No: 1) and instrumentation layout with index properties [17], (b) applied input motion

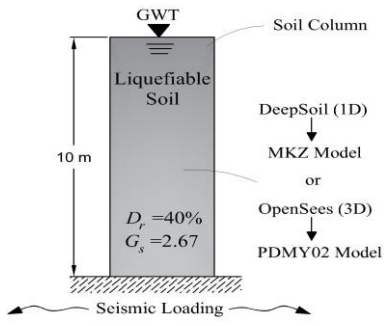

Figure 2. Schematic view of the simulated soil profile

Modulus reduction and damping curves of the soil were defined by using Darendeli [21] model for each layer in the soil column. MRDF with Darandeli reduction factor fitting tool was utilized to agree with the empirical nonlinear curves obtained from the Darendeli [21] curves.

Darendeli model requires five inputs that are plasticity index (PI), overconsolidation ratio (OCR), lateral earth pressure coefficient at rest (K_0), number of loading cycles (N_c), and frequency ($Freq$). The simulated soil was considered normally consolidated and non-plastic soil (OCR =1 and PI =0). N_c and $Freq$ were set 10 and 1.0 as recommended by [21], respectively. The value of K_0 was estimated using Jaky's [22] equation (Equation 1):

$$K_0 = 1 - sin\phi' \tag{1}$$

where effective friction angle, ϕ' =32° for D_r = 40% was considered from the empirical relationship given in [23].

Note that modulus reduction curves obtained from [21] are only valid for small shear strains (up to 0.3%). The implied shear strength procedure proposed by Hashash et al. [24] was applied to represent the real (target) shear strength of the soil for large shear strains. In this procedure, the original modulus reduction curve (G/G_{max}) for each layer computed from Darendeli's [21] equation was modified to reach target shear strength levels at large strains by adjusting the data points manually. The Mohr–Coulomb failure criterion was utilized to estimate the target shear strength of the soil ($\tau = \sigma' tan\phi + c'$, here c' assumed zero and ϕ' =32).

The soil profile was divided into 12 layers to ensure the frequency of each layer greater than 30 Hz which is the maximum frequency criteria recommended by [18]. The base of the soil profile was modeled as a rigid half-space. The shear wave velocity (V_s) of each soil layer was computed using Equation (2) that was generated from the resonant column test results performed by [25]. Figure 3 presents the distribution of V_s, maximum frequency, and implied friction angle with depth.

$$V_s = 99(z)^{0.25} \tag{2}$$

Vucetic and Dobry [26] model implemented in DeepSoil which was initially developed by Dobry et al. [27] and modified by Vucetic and Dobry [26] was used to estimate pore water pressure generation and dissipation of the soil used in the model as expressed in Equation (3):

$$r_{u,N} = \frac{pfN_cF(\gamma_c - \gamma_{tvp})^2}{1 + fN_cF(\gamma_c - \gamma_{tvp})} \tag{3}$$

where $r_{u,N}$ is residual pore water pressure ratio after N_c cycles; F, s, and p are the curve fitting parameters; f is equal to 1.0 or 2.0 depending on 1D or 2D shaking; γ_c is cyclic shear strain; γ_{tvp} is volumetric threshold shear strain. F is obtained to be 1.7 from the chart proposed by [28]. Similarly, s was assigned to be 1.0 based on [28]. p and γ_{tvp} was assumed as 1.15 and 0.05%, respectively. Table 1 summarizes all of the pore water pressure model parameters used in this study.

Two degradation indices proposed by Matasovic [19] were utilized in DeepSoil analyses (Equations 4 and 5) to simulate the shear strength and shear stiffness degradation of the soil depend on excess porewater pressure ratio:

$$\delta_G = \sqrt{1 - r_u} \tag{4}$$

$$\delta_\tau = 1 - (r_u)^v \tag{5}$$

in which δ_G and δ_τ are shear modulus and shear stress degradation functions, v is curve-fitting parameter. In this study, v =1.0 was used to better simulate the shear strength degradation.

In DeepSoil, the dissipation of excess pore water pressure is taken into account using Terzaghi's 1D consolidation theory. This theory requires the coefficient of consolidation (c_v) of the soil for evaluating pore water pressure dissipation. For Nevada sand, c_v of each layer was computed through Equation (6):

$$c_v = \frac{k(1 + e_0)}{\gamma_w a_v} \tag{6}$$

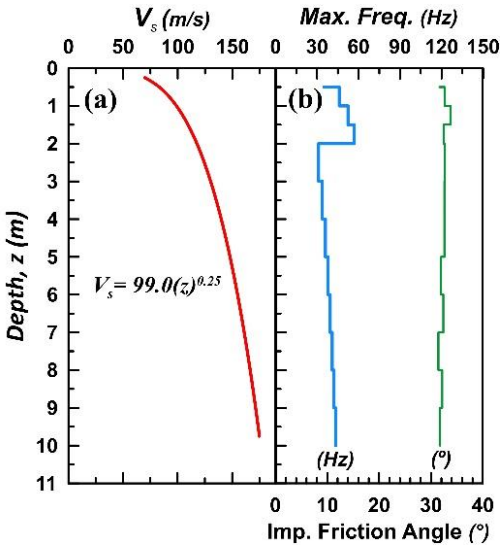

Figure 3. (a) V_s profile (b) maximum frequency and implied friction angle of the profile used in DeepSoil simulations

Table 1. Pore water pressure model parameters of the sand (D_r = 40%) used in simulations

	Value	Reference
F	1.7	[28]
s	1	[28]
p	1.15	-
f	1	-
γ_{tvp}	0.05	-
v	1	-
c_v	Equation (6)	-

In Equation 6, the symbol γ_w is the unit weight of the water and k is the permeability coefficient of the soil. e_0 is the initial void ratio, and a_v is the compressibility coefficient of the soil. k and e_0 was used to be 6.6x10^{-5} m/s and 0.74, respectively [25]. a_v was estimated using Equation (7) which was generated based on laboratory studies on Nevada sand by Gibson [29] (Figure 4). The coefficient of consolidation (c_v) of each soil layer was increased by 50 times due to the acceleration used in the centrifuge test.

$$a_v = 8.95\text{x}10^{-3}(\sigma'_v + 4.4)^{-0.93} \quad (7)$$

2.2 OpenSees

The open-source finite element (FE) analysis program OpenSees [30] was used to simulate the liquefiable soil behavior. The soil column was modeled using 3D eight-node brick elements. The element sizes of the model were suitably selected to be equal to or smaller than one-eighth of the minimum wavelength (λ_{min}) corresponding to the highest cut-off frequency (f_{max}) [31]. The 10 m soil profile was discretized in 1.0 m horizontal and 0.625 m vertical direction. At the bottom of the model was separately fixed in horizontal and vertical directions and formed as a rigid base to apply earthquake motion from this layer. Nodes at the same location on the lateral boundaries were tied to move together in all directions using equalDOF command in OpenSees.

Soil layers were constructed out of 8 node Brick UP elements to simulate fully coupled soil response. Each node has four degrees of freedom (DOFs), one for pore water pressure (p) and the others for translational displacements (u). An advanced constitutive model, Pressure Dependent Multi Yield02 (PDMY02) [32, 33] was employed to represent the nonlinear soil response. This material model is an elastoplastic model and can simulate the dilatancy and cyclic mobility behavior of sandy soils earthquake loading. The model uses a non-associative rule to define the dilative or contractive behavior of the soil.

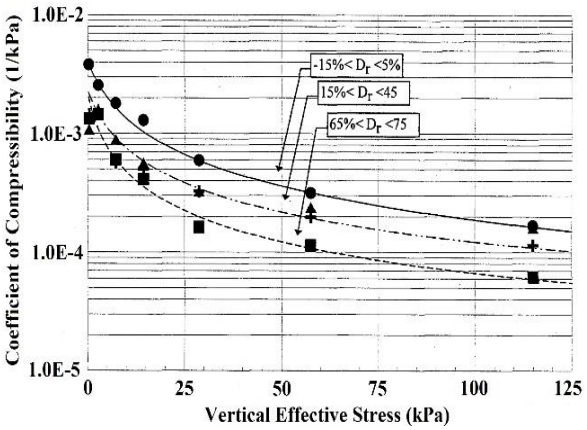

Figure 4. Variation of compressibility coefficients of Nevada Sand with vertical effective stress, [29]

The PDMY02 model has a total of 15 parameters and includes elastic, nonlinear and dilatancy properties, as listed in Table 2. Octahedral shear modulus of the soil ($G_{max,oct}$) were calculated using small strain shear modulus, $G_0 = \rho {V_s}^2$, as described in [34]. Bulk modulus of the soil (B_r) was derived from $G_{max,oct}$ and Poisson's ratio (ν). The default parameters were selected for $\gamma_{max,r}$, d , and NYS as suggested by Lu et al. [35]. Appropriate values was assigned for phase transformation angle (ϕ'_{pt}), contraction (c_1, c_2, c_3), and dilation parameters (d_1, d_2, d_3) as recommended by [30, 35].

Prior to seismic loading, static analysis was performed to apply the gravitational load and provide initial stress condition. Subsequently, the input motion was applied to the model by performing dynamic analysis. Simulations are carried with Rayleigh damping of 3% to apply low strain damping of the model. The Newmark integrator method was utilized to integrate the equations of motion.

3. Evaluation of Performance of Constitutive Soil Models

The performance of the numerical models to predict nonlinear liquefiable soil behavior was investigated through comparison of simulation and centrifuge test results. Comparison results were evaluated in terms of excess pore water pressure, acceleration-time history, spectral acceleration, and lateral displacement. In addition, maximum soil profile responses were presented to compare numerical simulation results and measured data throughout the soil profile.

Table 2. Selected PDMY02 model parameters during simulations

Parameter	Description	Value
ρ (ton/m^3)	Density	1.96
p_{ref} (kPa)	Reference effective confining stress	100
$G_{max,oct}$ (MPa)	Octahedral low-strain shear modulus	50
$\gamma_{max,r}$ (%)	Maximum octahedral shear strain	0.1
B_r (MPa)	Bulk modulus	122
d	Pressure dependency coefficient	0.5
c (kPa)	Cohesion	0.1
ϕ'_{txc}	Triaxial friction angle	32
ϕ'_{pt}	Phase transformation angle	27
c_1, c_2, c_3	Contraction and dilation coefficients	0.025, 4.5, 0.2
d_1, d_2, d_3		0.1, 3.0, 0.0
NYS	Number of yield surface	20

3.1 Excess Pore Water Pressure

The behavior of liquefiable soil is basically governed by the development and dissipation of excess pore pressures. Thus, it is important to adequately simulate excess pore pressures during seismic shaking to obtain the liquefiable soil behavior realistically.

Figure 5 shows measured and predicted excess pore pressures time histories at different locations. In general, MKZ (DeepSoil) and PDMY02 (OpenSees) models reasonably predicted the generation and dissipation of excess pore pressures at all depths.

3.2 Acceleration-Time Histories

Figure 6 compares acceleration-time histories results obtained from the measured and predicted data. Acceleration values predicted from numerical simulations are almost identical throughout the entire time history with the experimental study results, except amplitudes of accelerations. At the soil surface, numerical simulations overestimated the amplitude of accelerations to the centrifuge study. However, predicated acceleration-time histories were closer to measured data at 2.5 and 5 m depths. Besides, at 5 m depth, high dilation spikes were observed in the centrifuge test, while the phenomenon was not observed from predicted results.

3.3 Spectral Accelerations (S_a)

In Figure 7, measured and predicted spectral accelerations (S_a) at depths of 1.25, 2.5, and 5.0 m are presented. As seen from Figure 7, MKZ and PDMY02 models overestimated S_a values at the soil surface (AH3) between periods of 0.01 to 1.0s. As mentioned in Section 3.2, overestimation of S_a at the soil surface due to prediction of amplitude of accelerations higher than their experimental counterparts. On the other hand, two soil models showed a better match with centrifuge measurements at 2.5 and 5.0m depths as compared to soil surface records. Overall, the MKZ model exhibited better performance to predict spectral accelerations with respect to the PDMY02 model at three locations.

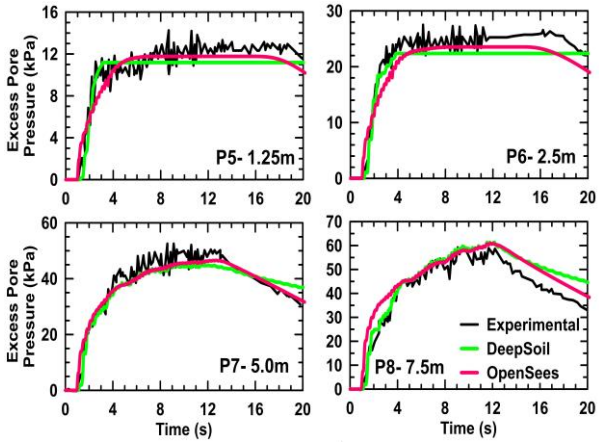

Figure 5. Comparison of excess pore water pressures obtained from numerical simulations and the centrifuge test

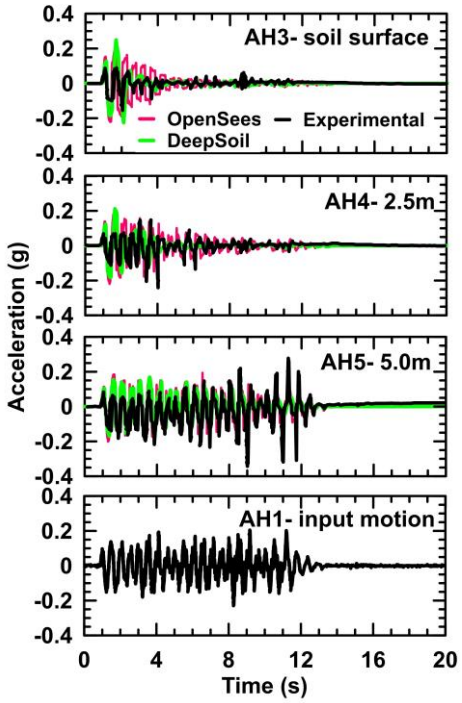

Figure 6. Variation of acceleration-time histories at different depths

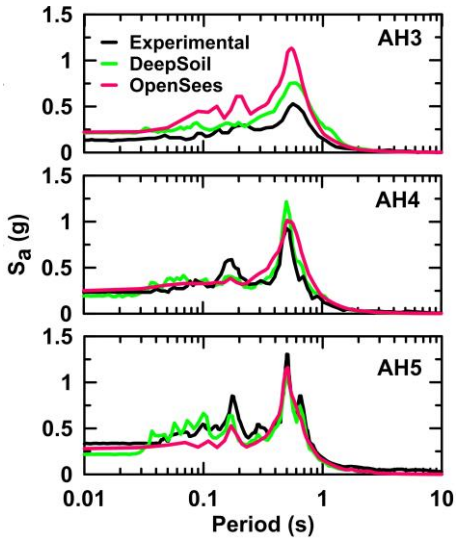

Figure 7. Comparison of simulated and measured spectral accelerations

Residual spectral accelerations were plotted for AH3, AH4, and AH5 to clearly assess the difference of the predicted spectral accelerations during the applied motion. Residuals of S_a between MKZ and PDMY02 models were computed in a logarithmic space as follows:

$$Residual\ S_a = \log \frac{S_{a,DeepSoil}}{S_{a,OpenSees}} \tag{8}$$

Positive values indicate that OpenSees (PDMY02) simulations underestimate S_a values with respect to DeepSoil (MKZ) ones, or vice versa. Figure 8 presents the residuals of spectral accelerations computed from numerical simulations.

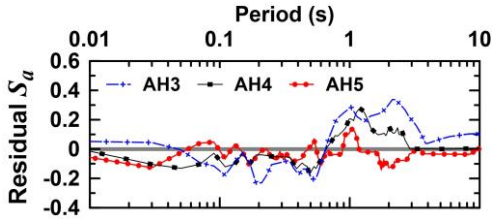

Figure 8. Residuals between the DeepSoil and OpenSees spectral accelerations (Sa)

During the simulations at 5.0 m depth (AH5), residual S_a was computed nearly zero for all periods which indicates that MKZ and PDMY02 models exhibited similar responses. On other hand, PDMY02 model overestimated spectral accelerations in periods between T=0.03-0.5s at the ground surface (AH3). Nevertheless, at high periods (low frequencies), spectral accelerations were underestimated from OpenSees simulations as compared to DeepSoil ones. At 2.5 m depth, PDMY02 model overestimated (negative residuals) S_a values up to T=0.5s, after that spectral accelerations were underestimated with respect to MKZ model predictions.

3.4 Lateral Displacements

Figure 9 compares lateral soil displacement results obtained from the centrifuge test and numerical simulations. The magnitude of predicted lateral displacements at each time step is consistent with the experimental measurements. In particular, MKZ model indicated more satisfactorily results with the experimental results as against PDMY02 model simulations.

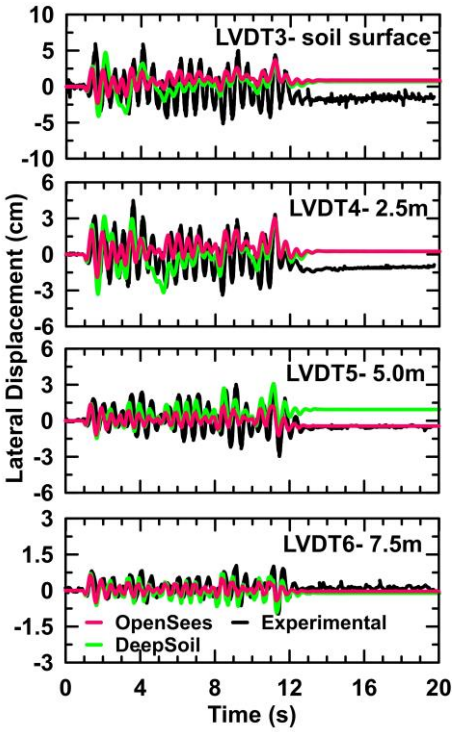

Figure 9. Variation of lateral displacements at different depths

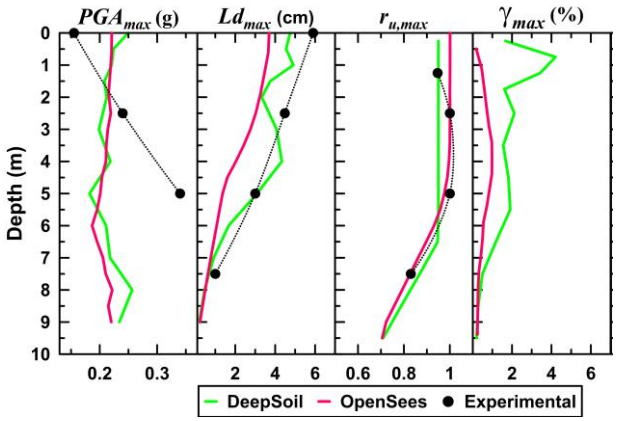

Figure 10. Maximum profile responses of numerical simulations and the centrifuge test

3.5 Maximum Profile Responses

Figure 10 compares the maximum profile response of numerical simulations in terms of maximum horizontal acceleration (PGA_{max}), maximum lateral displacements (Ld_{max}), maximum excess pore pressure ratio ($r_{u,max}$), and maximum shear strain (γ_{max}). The predicted PGA_{max} values from nonlinear DeepSoil analyses exhibited similar behavior with nonlinear OpenSees simulations through the soil profile. Nevertheless, numerical simulations generally underestimated the centrifuge results in terms of PGA_{max} except at soil surface measurement. At the soil surface, PGA_{max} values were overestimated from OpenSees (PDMY02) and DeepSoil (MKZ) simulations about 1.4 and 1.6 times smaller than the measured one, respectively. DeepSoil analyses provided a similar trend to the Ld_{max} measurements obtained from the centrifuge test but predicted Ld_{max} values from OpenSees simulations were about 37% lower than the measured Ld_{max} values. Besides, the predicted $r_{u,max}$ from numerical simulations were nearly the same to the experimental measurements. When compared the γ_{max} values obtained from numerical simulations, γ_{max} values increased up through the soil profile and reached the maximum value of 4.2% at about 1.0 m depth from DeepSoil analyses. However, computed maximum shear strains from OpenSees analyses were smaller than those obtained from DeepSoil analyses. The maximum shear strain was computed approximately γ_{max}= 1.0% at 4.0 m depth from OpenSees analyses.

4. Conclusions

In this paper, results from two different constitutive soil models were compared with centrifuge test measurements regarding their capability to predict one-layered liquefiable soil behavior with regard to excess pore water pressures, accelerations, lateral displacements, and maximum profile responses under a seismic shaking. The major findings from

this study are as follows:

- MKZ (DeepSoil) and PDMY02 (OpenSees) models are reasonable simulated generation and dissipation of excess pore pressures during seismic shaking when the calibration methodologies of the models are applied sufficiently.
- Acceleration-time histories and spectral accelerations at the ground surface were overestimated in both DeepSoil and OpenSees simulations. On the other hand, the predicted accelerations at deeper depths were in reasonable agreement with the centrifuge test results.
- DeepSoil model simulated the magnitudes of lateral displacements observed in the centrifuge experiment better than OpenSees ones. Similar results were obtained at different depths during maximum profile response simulations in terms of Ld_{max} and $r_{u,max}$.

The paper concluded that the models predict key responses of the liquefiable soil during seismic shaking. These models can be acceptably utilized to predict one-layered liquefiable soil behavior. Nevertheless, the MKZ model stands out in terms of properly predicting the relevant responses of the liquefiable soil and its simplicity in defining the input parameters as compared to the PDMY02 model. For future studies, the numerical models used in the current study should also be extended and validated for multi-layered soil profiles to evaluate liquefiable soil behavior accurately.

Declaration

The author declared no potential conflicts of interest with respect to the research, authorship, and/or publication of this article. The author also declared that this article is original, was prepared in accordance with international publication and research ethics, and ethical committee permission or any special permission is not required.

Author Contributions

S. Demir is responsible for all section of the study

Nomenclature

a_v : Compressibility coefficient
B_r : Bulk modulus of the soil
c' : Effective cohesion
c_1, c_2, c_3 : Contraction parameters
C_u : Coefficient of uniformity
d : Pressure dependence coefficient
d_1, d_2, d_3: Dilation parameters
D_r : Relative density
e_0 : Initial void ratio
f : Model constant
f_1, f_2 : Corner frequencies
f_{max} : Highest cut-off frequency
F, s, p : Curve fitting parameters
$Freq$: Frequency
$G_{max,oct}$: Octahedral shear modulus of the soil
G/G_{max} : Modulus reduction curve
k : Permeability
K_0 : Lateral earth pressure at rest
Ld_{max} : Maximum lateral displacement
NYS : Number of yield surface
N_c : Number of loading cycles
OCR : Over consolidation ratio
PGA_{max} : Maximum horizontal acceleration
PI : Plasticity index
p : Pore water pressure
p_{ref} : Reference effective confining stress
r_u : Excess pore water pressure ratio
$r_{u,max}$: Maximum excess pore water pressure ratio
$r_{u,N}$: Residual pore water pressure ratio after N_c cycles
u : Displacement
v : Curve-fitting parameter
V_s : Shear wave velocity
β, γ : Parameters for integrator Newmark
δ_G : Shear modulus degradation function
δ_G : Shear stress degradation function
ϕ' : Effective friction angle
ϕ'_{txc} : Triaxial friction angle
ϕ'_{pt} : Phase transformation angle
γ_c : Cyclic shear strain
γ_{max} : Maximum shear strain
$\gamma_{max,r}$: Maximum octahedral shear strain
γ_{tvp} : Volumetric threshold shear strain
γ_w : Unit weight of the water
λ_{min} : Minimum wavelength
ν : Poisson's ratio
σ' : Effective stress
ρ : Saturated mass density

References

1. Kramer, S. and A. Elgamal, *Modeling soil liquefaction hazards for performance based earthquake engineering. Report 2001/13, Pacific Earthquake Engineering Research Center.* University of California, Berkeley, 2001. p.165
2. Kramer, S.L., *Geotechnical earthquake engineering*. Prentice-Hall Civil Engineering and Engineering Mechanics Series. 1996, Upper Saddle River, NJ: Pearson 653.
3. Popescu, R. and J.H. Prevost, *Centrifuge validation of a numerical model for dynamic soil liquefaction.* Soil Dynamics and Earthquake Engineering, 1993. **12**(2): p. 73-90.
4. Byrne, P.M., Park, S.S., Beaty, M., Sharp, M., Gonzalez, L. and Abdoun, T., *Numerical modeling of liquefaction and comparison with centrifuge tests.* Canadian Geotechnical Journal, 2004. **41**(2): p. 193-211.
5. Taiebat, M., H. Shahir, and A. Pak, *Study of pore pressure variation during liquefaction using two constitutive models for sand.* Soil Dynamics and Earthquake Engineering, 2007. **27**(1): p. 60-72.
6. Ramirez, J., et al., *Site response in a layered liquefiable deposit: evaluation of different numerical tools and methodologies with centrifuge experimental results.* Journal of Geotechnical and Geoenvironmental Engineering, 2018. **144**(10): p. 1-22.

7. Demir, S. and P. Özener, *Estimation of Liquefaction with UBC3D-PLM Model: A Centrifuge Test Example.* Teknik Dergi, 2019. **30**(5): p. 9421-9442.
8. Prevost, J.H., *A simple plasticity theory for frictional cohesionless soils.* International Journal of Soil Dynamics and Earthquake Engineering, 1985. **4**(1): p. 9-17.
9. Matasović, N. and M. Vucetic, *Cyclic characterization of liquefiable sands.* Journal of Geotechnical Engineering, 1993. **119**(11): p. 1805-1822.
10. Beaty, M. and P.M. Byrne, *An Effective Stress Model for Pedicting Liquefaction Behaviour of Sand*. in *Geotechnical Earthquake Engineering and Soil Dynamics III*. 1998. ASCE. pp. 766-777
11. Yang, Z., A. Elgamal, and E. Parra, *Computational model for cyclic mobility and associated shear deformation.* Journal of Geotechnical and Geoenvironmental Engineering, 2003. **129**(12): p. 1119-1127.
12. Dafalias, Y.F. and M.T. Manzari, *Simple plasticity sand model accounting for fabric change effects.* Journal of Engineering mechanics, 2004. **130**(6): p. 622-634.
13. Petalas, A. and V. Galavi, *Plaxis Liquefaction Model UBC3DPLM.* Plaxis Report, 2013.
14. Ziotopoulou, K. and R. Boulanger, *Calibration and implementation of a sand plasticity plane-strain model for earthquake engineering applications.* Soil Dynamics and Earthquake Engineering, 2013. **53**: p. 268-280.
15. Khosravifar, A., Elgamal, A., Lu, J. and Li, J., *A 3D model for earthquake-induced liquefaction triggering and post-liquefaction response.* Soil Dynamics and Earthquake Engineering, 2018. **110**: p. 43-52.
16. Yang, M., M. Taiebat, and Y. Dafalias, *A New Sand Constitutive Model for Pre-and Post-liquefaction Stages*. in *International Conference of the International Association for Computer Methods and Advances in Geomechanics*. IACMAG 2021. **129**:p. 718-726.
17. Taboada, V. and R. Dobry, *Experimental results of model no. p. 1 at RPI*, in *Arulanandan K, Scott RF, editors. Verification of numerical procedures for the analysis of soil liquefaction problems*. 1993, Rotterdam, A.A. Balkema. p. 3-18.
18. Hashash, Y.M., et al., *DEEPSOIL 7.0, User Manual. Urbana, IL, Board of Trustees of University of Illinois at Urbana-Champaign.* 2016. p. 170.
19. Matasovic, N., *Seismic response of composite horizontally-layered soil deposits*. 1993, University of California. p. 452.
20. Phillips, C. and Y.M. Hashash, *Damping formulation for nonlinear 1D site response analyses.* Soil Dynamics and Earthquake Engineering, 2009. **29**(7): p. 1143-1158.
21. Darendeli, M.B., *Development of a new family of normalized modulus reduction and material damping curves*, in *Civil Engineering*. 2001, University of Texas at Austin. p. 362.
22. Jaky, J., *The coefficient of earth pressure at rest.* J. of the Society of Hungarian Architects and Engineers, 1944: p. 355-358.
23. Meyerhof, G.G., *Compaction of sands and bearing capacity of piles.* Transactions of the American Society of Civil Engineers, 1959. **126**(1): p. 1292-1322.
24. Hashash, Y., C. Phillips, and D.R. Groholski, *Recent advances in non-linear site response analysis.* in *5th Int. Conf. in Recent Advances in Geotechnical Earthquake Engineering and Soil Dynamics*. 2010. Missouri Univ. of Science and Technology, Rolla, MO. p. 1-22.
25. Arulmoli, K., Muraleetharan, K. K., Hossain, M. M. and Fruth, L. S., *VELACS: Verification of liquefaction analyses by centrifuge studies, laboratory testing program.* Soil data report, 1992.
26. Vucetic, M. and R. Dobry, *Pore pressure build-up and liquefaction at level sandy sites during earthquakes*. 1986: Research Rep. No. CE-86-3. Troy, NY: Dept. of Civil Engineering, Rensselaer Polytechnic Institute. p. 616.
27. Dobry, R., Pierce, W.G., Dyvik, R., Thomas, G.E. and Ladd, R.S., *Pore pressure model for cyclic straining of sand*, in *Rensselaer Polytechnic Institute, Troy, New York.* 1985: Research Report 1985-06.
28. Mei, X., S.M. Olson, and Y.M. Hashash, *Empirical porewater pressure generation model parameters in 1-D seismic site response analysis.* Soil Dynamics and Earthquake Engineering, 2018. **114**: p. 563-567.
29. Gibson, A.D., *Physical scale modeling of geotechnical structures at one-G*. 1997, California Institute of Technology. p. 397.
30. Mazzoni, S., McKenna F, Scott M.H, and Fenves G.L., *Open system for earthquake engineering simulation user command-language manual—OpenSees version 2.0.* Pacific Earthquake Engineering Research Center, Univ. of California, Berkeley, CA, 2009. p. 451.
31. Kuhlemeyer, R.L. and J. Lysmer, *Finite element method accuracy for wave propagation problems.* Journal of Soil Mechanics & Foundations Div, 1973. **99**(5): p.421-427.
32. Parra, E., *Numerical modeling of liquefaction and lateral ground deformation including cyclic mobility and dilative behavior in soil systems*. 1996, Department of Civil Engineering, Rensselaer Polytechnic Institute, Troy, NY.
33. Yang, Z., J. Lu, and A. Elgamal, *OpenSees soil models and solid-fluid fully coupled elements user's manual.* 2008. p. 1-25.
34. Khosravifar, A., *Analysis and design for inelastic structural response of extended pile shaft foundations in laterally spreading ground during earthquakes*. 2012, University of California, Davis. p. 310.
35. Lu, J., A. Elgamal, and Z. Yang, *OpenSeesPL: 3D lateral pile-ground interaction user manual (Beta 1.0).* Department of Structural Engineering, University of California, San Diego, 2011. p. 147.